JACS
JOURNAL OF THE AMERICAN CHEMICAL SOCIETY

Communication

pubs.acs.org/JACS

Highly Adaptable Two-Dimensional Metal–Organic Coordination Networks on Metal Surfaces

Christopher S. Kley,*[,†] Jan Čechal,[†] Takashi Kumagai,[†] Frank Schramm,[‡] Mario Ruben,*[,‡,§] Sebastian Stepanow,*[,†] and Klaus Kern[†,∥]

[†]Max-Planck-Institut für Festkörperforschung, Heisenbergstrasse 1, D-70569 Stuttgart, Germany

[‡]Institut für Nanotechnologie, Karlsruhe Institute of Technology, Hermann-von-Helmholtz-Platz 1, 76344 Eggenstein-Leopoldshafen, Germany

[§]Strasbourg Institute of Material Physics and Chemistry, Centre National de la Recherche Scientifique, Unité Mixte de Recherche 7504, Université de Strasbourg, 23 Rue du Loess, 67034 Strasbourg, France

[∥]Institut de Physique de la Matière Condensée, École Polytechnique Fédérale de Lausanne, 1015 Lausanne, Switzerland

Supporting Information

ABSTRACT: The formation of extended two-dimensional metal–organic coordination networks (2D-MOCNs) showing high adaptability to surface step edges and structural defects is revealed by scanning tunneling microscopy. Rod-like 4,4′-di-(1,4-buta-1,3-diynyl)-benzoic acid (BDBA) and iron atoms assemble into extended 2D-MOCNs on Au(111) and Ag(100) surfaces. Independent from the chosen substrate and its surface symmetry the MOCN grows continuously over multiple surface terraces through mutual in-phase structure adaptation of network domains at step edges as well as on terraces. The adaptability of the MOCNs is mainly ascribed to the high degree of conformational flexibility of the butadiynyl functionality of the ligand. Despite their flexibility, the MOCNs exhibit considerable robustness against annealing at high temperatures. The findings show that mesoscale self-assembled functional architectures with a high degree of substrate error tolerance can be realized with metal coordination networks.

Supramolecular assembly of surface-confined 2D-architectures is a topic of intense research with potential applications in surface patterning,[1−3] catalytic model systems,[4,5] molecular electronics, and spintronics.[6,7] In particular, surface-assisted metal-coordination bonding allows the synthetic bottom-up fabrication of molecular architectures of well-defined geometry with specific functional properties. Many examples of diverse metal–organic coordination networks (MOCNs) with tunable sizes and topologies,[8] suitable for host–guest chemistry,[9,10] and regular arrays of spin centers[11] were demonstrated. Moreover, 2D metal–organic superlattices with a high degree of structural order up to the micrometer range were reported.[12] Recently, on-surface covalent polymer networks have gained increasing attention as a route to pattern surfaces with molecular adlayers due to their high thermal and chemical stability.[13−19] However, in contrast to MOCNs, the structural control of polymer networks is limited by the presence of radical and highly reactive intermediates during the assembly process and the exclusion of error correction in the irreversible formation of covalent bonds. MOCNs, on the other hand, show self-selection and error correction as demonstrated by a heteroleptic bonding motif due to the specific binding of the ligands to the metal centers.[8] Apart from separated examples of graphene and hexagonal boron nitride layers, one common obstacle of both MOCNs and polymer networks is the limitation of the mesoscale ordering imposed by substrate step edges. Recently, the assembly of several hundred nanometer long one-dimensional molecular chains driven by hydrogen bonds showing crossing over step edges was observed on one specific substrate and surface symmetry.[20,21] However, 2D-MOCNs were not observed to show insensitivity to native surface steps and defects.

Here we address the challenge of designing 2D-MOCNs that overcome the limitations imposed by surface steps. To this end, we have synthesized the rod-like ligand 4,4′-di-(1,4-buta-1,3-diynyl)-benzoic acid (BDBA), which is schematically depicted in Figure 1. Sample preparation and characterization were conducted in two ultrahigh vacuum systems equipped with a home-built variable temperature and a low-temperature scanning tunneling microscope (STM). The base pressure of both systems is better than 3×10^{-10} mbar. Single crystal Au(111) and Ag(100) surfaces were prepared by repeated cycles of Ar^+ sputtering and annealing at 800 K. BDBA molecules and iron atoms were deposited simultaneously in situ by organic molecular beam epitaxy from a quartz crucible heated to 560 K and an electron-beam heated evaporator, respectively. During deposition the substrate temperature was held in the range of 450–460 K. STM data were recorded in

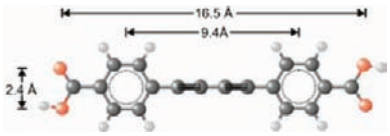

Figure 1. Chemical structure of the 4,4′-di-(1,4-buta-1,3-diynyl)-benzoic acid with carboxylic and alkynyl functionalities (H, white; C, gray; O, red).

Received: December 16, 2011
Published: March 29, 2012

ACS Publications © 2012 American Chemical Society

dx.doi.org/10.1021/ja211749b | J. Am. Chem. Soc. 2012, 134, 6072–6075

constant current mode after the sample was cooled to room temperature or 5 K, respectively. A detailed description of the preparation procedure is given in the Supporting Information (SI).

Figure 2a,c depicts two representative STM images with 2D-MOCNs on Au(111) and Ag(100) surfaces, respectively. The network formation is controlled by the metal-to-molecule concentration ratio (see SI). At the employed Fe:BDBA ratio of 1:1, fully reticulated network structures form comprising iron dimers at the network nodes as demonstrated in Figure 2b. At each network node four BDBA molecules coordinate with their carboxylate groups to Fe adatoms in two different modes. Two BDBA molecules bridge the diiron unit symmetrically while each of the other two axial ligands forms bidentate bonds to one Fe atom of the dimer. An asymmetric configuration with monodendate axial ligands was also observed.

Similar networks and binding motifs were reported in previous works on Fe-carboxylate coordination systems.[22−25] However, in contrast to previous findings the orientation of the Fe dimers shows a mixed phase of parallel and alternating arrangements with no strict periodicity. Apart from the similarities of the local structural details of the networks with other Fe-carboxylate systems, the BDBA-Fe MOCNs exhibit a high insensitivity to step edges of various shapes and orientations, i.e., the network extends over surface steps without breaking the network integrity. At the step edges, BDBA-Fe domains originating from adjacent surface terraces mutually adapt in-phase resulting in the extension of the network structure over multiple surface steps (cf. Figure 2a,c).

The Fe dimer orientation, spacing, and local ligand arrangement exhibit a broad range of geometries that becomes apparent in Figure 2b. The BDBA is capable of undergoing internal conformational changes as demonstrated in the middle and right image of Figure 2b. Here, several ligands are strongly bent while coordinating to iron atoms in the network. In addition, network triangles and pentagons can be identified at the domain interfaces. The strong variations of the ligand adsorption geometry deviating from the high-symmetry directions of the underlying surface are accompanied by a high degree of flexibility at the coordination centers of the network.[8] These highly irregular transition structures of the ligand as well as the flexibility of the coordination bonding enable the mutual adaptation of BDBA-Fe domains growing on the same terrace with different orientations. Both, the flexibility of the metal−ligand bond and the conformational freedom of the molecules result in an overall fully reticulated network that lacks strict 2D periodicity. In contrast to the metal−ligand bond flexibility found in heteroleptic MOCNs[8] the error tolerance and adaptability of the presented homoleptic network are a consequence of the high flexibility of the chemisorbed ligands and shows, in contrast to former works, also high insensitivity to step edges as presented in the following.[8,22−24]

Figure 3 demonstrates in more detail the flexibility and adaptability of the BDBA molecules at Au(111) and Ag(100) step edges. Figure 3a shows an MOCN extending over a step edge. BDBA decorates the step edge with its long axis oriented along the step direction at the lower side of the step. Ligand molecules of adjacent terraces point to a common network node across the step edge with the upper ligand apparently extending over the step. The variations in the apparent heights of the ligands in the STM images in Figure 3a,c indicate that the step molecules can adopt different configurations. We interpret this observation as the molecules' ability to reside flat at the lower side of the step or, when closer to the step, to adopt a tilted or bent configuration. Figure 3b illustrates the ability to form continuous networks on a rugged Ag(100) surface. A fully reticulated MOCN extending over multiple steps was observed. However, it is likely that during the

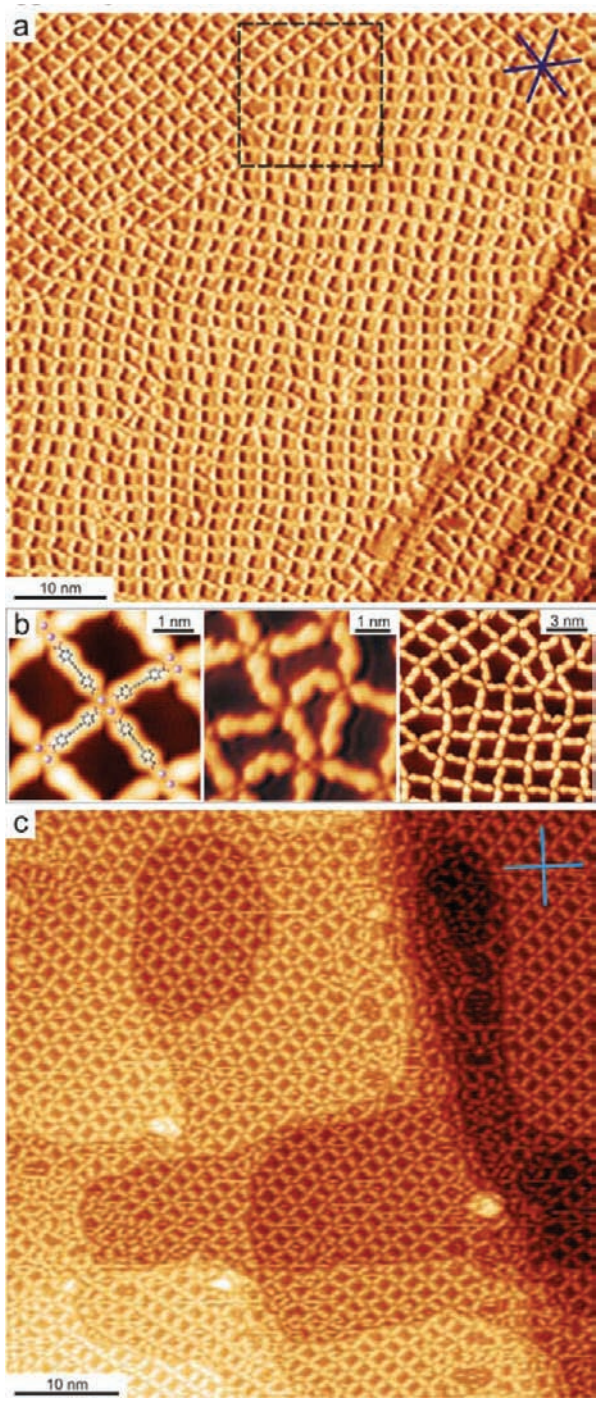

Figure 2. Representative STM images of BDBA-Fe MOCNs. The close-packed substrate directions are indicated by blue crosses. (a) Au(111). Individual network domains adapt both at surface steps and on terraces. (b) The left image shows a regular network with the central di-iron binding motif. The middle image shows ligands in a bent configuration. The right image shows the mutual adaptation of two domains on the same terrace. The conformational adaptation of the molecules and the formation of irregular triangular and pentagonal network structures can be observed (Au(111), 5 K, −0.6 V, 0.3 nA). (c) Ag(100). The MOCN is formed over multiple step edges of various shapes and adapts to subtle substrate variations (297 K, −0.9 V, 0.08 nA).

dx.doi.org/10.1021/ja211749b | J. Am. Chem. Soc. 2012, 134, 6072−6075

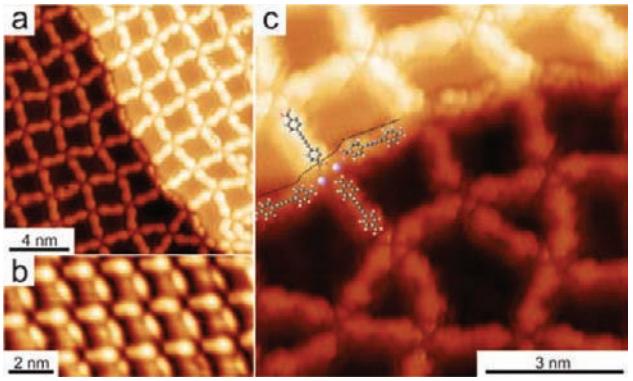

Figure 3. High-resolution STM topographs of BDBA-Fe MOCNs. (a) Fully reticulated network crossing a Au(111) step (5 K, 0.8 V, 0.7 nA). The domains at the lower and upper terrace mutually adapt and merge in-phase at an irregularly shaped step edge. Iron dimer centers were resolved except at the direct step edge region. (b) Continuous BDBA-Fe network on a rugged Ag(100) surface (5 K, −0.9 V, 0.5 nA). (c) BDBA-Fe at a Au(111) step edge (5 K, 0.8 V, 0.3 nA). The submolecular resolution exhibits the configurational degree of freedom of the edge molecules.

network formation the steps are reconstructed on the Ag(100) surface (see also SI).

As demonstrated above, the BDBA exhibits a high degree of conformational and orientational flexibility. The ability of the BDBA to assume different adsorption geometries including strongly bent and titled configurations is ascribed to its butadiyne backbone. In general the sp bonded alkynyl structure exhibits only limited bond angle flexibility. However, the asymmetric interaction of the orthogonal π-orbitals with the surface may lead to a partial rehybridization including higher sp^n orbitals, thus altering the 180° bond angle. A potential charge transfer to the π^* orbital could effectively lower the bond order of the alkyne carbon atoms. On the other hand, in the absence of Fe atoms the pristine BDBA molecule does not exhibit variations from its rod-like shape. In this case, neither intramolecular bending nor strong adsorption site variation were observed on both Ag(100) and Au(111) surfaces (see SI).[26] The estimated binding energy for Fe-carboxylate networks in similar 2D configurations amounts to about 1.2 eV per bond.[27] We reason that the energy gain from the coordination bond formation overcompensates the energy expense for the bending of the molecules, thus enabling the adaptation ability of the network.

The position and orientation of the Fe dimers and ligands relative to the substrate lattice is determined by the dominant BDBA-Fe coordination. The network structure exhibits a broad range of nonequivalent adsorption sites and orientations for both the iron dimers and ligands (see statistical analysis in SI). This is a result of many different possible bonding and adsorption configurations that are energetically accessible. These observations are in contrast to Fe-carboxylate networks with rigid polyphenyl ligands, where the network orientation, molecular adsorption, and the position of the iron atoms is well determined with only little structural variations.[22−25,27] However, the use of a less rigid 2-fold coordination motif can result in highly flexible 1D chains.[19]

The crossing of the network structure at the step edges follows predominantly one motif as indicated by the tentative model of the local configuration superposed in Figure 3c. Two axial ligands are generally adsorbed directly parallel at the step edge. The two molecules perpendicular to the step form bridging bonds to the Fe dimer with the upper ligand extending somewhat over the terrace step which is enabled by the flexibility of the ligand backbone. In previous work ditopic rod-like dicarboxylic acids also extend with the carboxyl moiety over the step edge. In that case however, the carboxylic acid remained protonated forming hydrogen bonded molecular chains with no metal adatom involved in the bonding.[14] Here, we can rule out the possibility of protonated molecules by the presence of reactive Fe metal adatoms and thermally induced deprotonation of the carboxylic group upon annealing (see SI). The in-phase crossing of surface steps was not observed for related Fe-polyphenyl carboxylate networks, which we ascribe to the low flexibility of these ligands.[8,9,22−25,27]

The variations in the Fe dimer configurations are inherently linked to their imaging by STM. Even under suitable tip conditions, parts of the MOCN with visible iron dimers coexisted with network parts where the iron could not be resolved. We ascribe this to local electronic differences due to different coordination geometries. In this context, the iron centers were not resolved in the direct step edge region. However, we expect the presence of iron dimers in the coordination nodes at the lower side of the step edges from the analysis of the ligand arrangement and distances. At the step edge, the metal−ligand bond distances for both the bridging and axial molecules are in accordance with corresponding distances found on surface terraces (for further analysis see SI).

In the absence of iron atoms, i.e., in the molecular phase of BDBA, this bonding motif and step edge crossing was never observed, neither on terraces nor at step edges of Ag(100) and Au(111) surfaces (see SI). The necessity of iron atoms indicates that neither silver nor gold adatoms are incorporated in the MOCN nodes. In comparison to the hydrogen-bonded one-dimensional molecular chains, density functional theory calculations show that the binding energy is dominated by hydrogen bonds with interaction strengths larger than the inclusion of substrate adatoms or step atoms.[14] With respect to metal−ligand interactions this supports the incorporation of iron atoms in the coordination nodes and the exclusion of surface adatoms in the nodes.

Upon thermal activation during the MOCN formation process the Ag(100) surface morphology appears to be reconstructed in certain areas (cf. Figure 3b).[28] On each terrace a single BDBA molecule coordinates with its carboxylate groups to iron dimers at opposite steps. Although this configuration is only rarely observed, the terraces appear to be modified for the accommodation of one molecule. The metal−ligand interactions are hereby combined with the surface reshaping (see also SI). It is worth noting that the MOCNs on both Au(111) and Ag(100) surfaces are robust against annealing to at least 490 K.

In conclusion, we have demonstrated the self-assembly of extended metal−organic coordination networks, which grow continuously over multiple surface steps showing a high degree of insensitivity and adaptability to intrinsic surface defects. This is enabled by the conformational flexibility of the butadiyne backbone forming bond angles far from ideal, hence conferring a high degree of error tolerance to the ligand molecules. Our findings are valid on both silver and gold substrates with different surface symmetries. Further, the MOCNs are distinguished by their considerable thermal robustness.

The high degree of substrate error tolerance of the MOCNs enables the realization of large-scale 2D-MOCNs. Particularly, our findings open up the way to pattern also rough and

imperfect surfaces, e.g., small crystallites, with regular and thermally stable metal−organic structures. These MOCNs with high surface coverage can be further functionalized for diverse applications by making use of the butadiynyl moieties for the selective binding of guest species.

■ ASSOCIATED CONTENT

Supporting Information

(1) Preparation details of the organic ligand 4,4′-di-(1,4-buta-1,3-diynyl)-benzoic acid (BDBA). (2) MOCN preparation method. (3) BDBA molecular phases on Au(111) and Ag(100). (4) BDBA-Fe networks on Au(111) and Ag(100). (5) Statistical analysis of the ligand orientations within the MOCNs on Au(111) and Ag(100). (6) Iron dimer coordination binding motifs on Ag(100) and Au(111). (7) References. This material is available free of charge via the Internet at http://pubs.acs.org.

■ AUTHOR INFORMATION

Corresponding Author

c.kley@fkf.mpg.de; mario.ruben@kit.de; s.stepanow@fkf.mpg.de

Notes

The authors declare no competing financial interest.

■ ACKNOWLEDGMENTS

This work was supported by the Baden-Württemberg Stiftung. J.Č. acknowledges the support of a Marie Curie Intra-European Fellowship of the 7th FP (AdaptNano, Project No. 251930) and CEITEC (CZ.1.05/1.1.00/02.0068). T.K. acknowledges the support of JSPS (Japan Society for the Promotion of Science).

■ REFERENCES

(1) Cicoira, F.; Santato, C.; Rosei, F. *Top. Curr. Chem.* **2008**, *285*, 203−267.
(2) Bartels, L. *Nat. Chem.* **2010**, *2*, 87−95.
(3) Barth, J. V.; Costantini, G.; Kern, K. *Nature* **2005**, *437*, 671−679.
(4) Seufert, K.; Bocquet, M.-L.; Auwärter, W.; Weber-Bargioni, A.; Reichert, J.; Lorente, N.; Barth, J. V. *Nat. Chem.* **2011**, *3*, 114−119.
(5) Fabris, S.; Stepanow, S.; Lin, N.; Gambardella, P.; Dmitriev, A.; Honolka, J.; Baroni, S.; Kern, K. *Nano Lett.* **2011**, *11*, 5414−5420.
(6) Carbone, C.; et al. *Adv. Funct. Mater.* **2011**, *21*, 1212−1228.
(7) Urdampilleta, M.; Klyatskaya, S.; Cleuziou, J.-P.; Ruben, M.; Wernsdorfer, W. *Nat. Mater.* **2011**, *10*, 502−506.
(8) Langner, A.; Tait, S. L.; Lin, N.; Rajadurai, C.; Ruben, M.; Kern, K. *Proc. Natl. Acad. Sci. U.S.A.* **2007**, *46*, 17927−17930.
(9) Stepanow, S.; Lingenfelder, M.; Dmitriev, A.; Spillmann, H.; Delvigne, E.; Lin, N.; Deng, X.; Cai, C.; Barth, J. V.; Kern, K. *Nat. Mater.* **2004**, *3*, 229−233.
(10) Kühne, D.; Klappenberger, F.; Krenner, W.; Klyatskaya, S.; Ruben, M.; Barth, J. V. *Proc. Natl. Acad. Soc. U.S.A.* **2010**, *107*, 21332−21336.
(11) Gambardella, P.; et al. *Nat. Mater.* **2009**, *8*, 189.
(12) Kühne, D.; Klappenberger, F.; Decker, R.; Schlickum, U.; Brune, H.; Klyatskaya, S.; Ruben, M.; Barth, J. V. *J. Am. Chem. Soc.* **2009**, *131*, 3881−3883.
(13) Méndez, J.; López, M. F.; Martín-Gago, J. A. *Chem. Soc. Rev.* **2011**, *40*, 4578−4590.
(14) Bieri, M.; Nguyen, M.-T.; Gröning, O.; Cai, J.; Treier, M.; Aït-Mansour, K.; Ruffieux, P.; Pignedoli, C. A.; Passerone, D.; Kastler, M.; Müllen, K.; Fasel, R. *J. Am. Chem. Soc.* **2010**, *132*, 16669−16676.
(15) Abel, M.; Clair, S.; Ourdjini, O.; Mossoyan, M.; Porte, L. *J. Am. Chem. Soc.* **2011**, *133*, 1203−1205.
(16) Bieri, M.; et al. *Chem. Commun.* **2009**, *45*, 6919−6921.
(17) Perepichka, D. F.; Rosei, F. *Science* **2009**, *323*, 216−217.
(18) Zwaneveld, N. A. A.; Pawlak, R.; Abel, M.; Catalin, D.; Gigmes, D.; Bertin, D.; Porte, L. *J. Am. Chem. Soc.* **2008**, *130*, 6678−6679.
(19) Heim, D.; Écija, D.; Seufert, K.; Auwärther, W.; Aurisicchio, C.; Fabbro, C.; Bonifazi, D.; Barth, J. V. *J. Am. Chem. Soc.* **2010**, *132*, 6783−6790.
(20) Schnadt, J.; Rauls, E.; Xu, W.; Vang, R. T.; Knudsen, J.; Lægsgaard, E.; Li, Z.; Hammer, B.; Besenbacher, F. *Phys. Rev. Lett.* **2008**, *100*, 046103.
(21) Schnadt, J.; Xu, W.; Vang, R. T.; Knudsen, J.; Zheshen, L.; Lægsgaard, E.; Besenbacher, F. *Nano Res.* **2010**, *3*, 459−471.
(22) Dmitriev, A.; Spillmann, H.; Lin, N.; Barth, J. V.; Kern, K. *Angew. Chem., Int. Ed.* **2003**, *42*, 2670−2673.
(23) Lingenfelder, M. A.; Spillmann, H.; Dmitriev, A.; Stepanow, S.; Lin, N.; Barth, J. V.; Kern, K. *Chem.—Eur. J.* **2004**, *10*, 1913−1919.
(24) Stepanow, S.; Lin, N.; Barth, J. V.; Kern, K. *J. Phys. Chem. B* **2006**, *110*, 23472−23477.
(25) Zhang, Y.-F.; Zhu, N.; Komeda, T. *J. Phys. Chem. C* **2007**, *111*, 16946−16950.
(26) Stuve, E. M.; Madix, R. J.; Sexton, B. A. *Surf. Sci.* **1982**, *123*, 491−504.
(27) Clair, S.; Pons, S.; Fabris, S.; Baroni, S.; Brune, H.; Kern, K.; Barth, J. V. *J. Phys. Chem. B* **2006**, *110*, 5627−5632.
(28) Pascual, J. I.; Barth, J. V.; Ceballos, G.; Trimarchi, G; De Vita, A.; Kern, K.; Rust, H.-P. *J. Chem. Phys.* **2004**, *120* (24), 11367−11370.